p27 transcriptionally coregulates cJun to drive programs of tumor progression

Hyunho Yoon[a,1], Minsoon Kim[a,b,1], Kibeom Jang[a,b], Miyoung Shin[a], Alexandra Besser[a,c], Xue Xiao[d], Dekuang Zhao[a], Seth A. Wander[a], Karoline Briegel[a,e], Lluis Morey[a,f,g], Andy Minn[h,i], and Joyce M. Slingerland[a,b,c,f,j,2]

[a]Braman Family Breast Cancer Institute, Sylvester Comprehensive Cancer Center, University of Miami Miller School of Medicine, Miami, FL 33136; [b]Department of Biochemistry and Molecular Biology, University of Miami Miller School of Medicine, Miami, FL 33136; [c]Sheila and David Fuente Graduate Program in Cancer Biology, University of Miami Miller School of Medicine, Miami, FL 33136; [d]Bioinformatics Core, Sylvester Comprehensive Cancer Center, University of Miami Miller School of Medicine, Miami, FL 33136; [e]Department of Surgery, University of Miami Miller School of Medicine, Miami, FL 33136; [f]Cancer Epigenetics Program, Sylvester Comprehensive Cancer Center, University of Miami Miller School of Medicine, Miami, FL 33136; [g]Department of Human Genetics, University of Miami Miller School of Medicine, Miami, FL 33136; [h]Department of Radiation Oncology, Perelman School of Medicine, University of Pennsylvania, Philadelphia, PA 19104; [i]Abramson Family Cancer Research Institute, Perelman School of Medicine, University of Pennsylvania, Philadelphia, PA 19104; and [j]Department of Medicine, University of Miami Miller School of Medicine, Miami, FL 33136

Edited by Joan S. Brugge, Harvard Medical School, Boston, MA, and approved February 13, 2019 (received for review October 10, 2018)

p27 shifts from CDK inhibitor to oncogene when phosphorylated by PI3K effector kinases. Here, we show that p27 is a cJun coregulator, whose assembly and chromatin association is governed by p27 phosphorylation. In breast and bladder cancer cells with high p27pT157pT198 or expressing a CDK-binding defective p27pT157pT198 phosphomimetic (p27CK−DD), cJun is activated and interacts with p27, and p27/cJun complexes localize to the nucleus. p27/cJun up-regulates *TGFB2* to drive metastasis in vivo. Global analysis of p27 and cJun chromatin binding and gene expression shows that cJun recruitment to many target genes is p27 dependent, increased by p27 phosphorylation, and activates programs of epithelial–mesenchymal transformation and metastasis. Finally, human breast cancers with high p27pT157 differentially express p27/cJun-regulated genes of prognostic relevance, supporting the biological significance of the work.

p27 | cJun | EMT | TGF-β2 | transcriptional regulation

The CDK inhibitor, p27, was discovered as a mediator of growth arrest by transforming growth factor type β (TGF-β) that impedes cell cycle progression by inhibiting cyclin-dependent kinases (CDKs) (1–3). p27 is invariably deregulated in human cancers, but unlike typical tumor suppressors, mutations or deletions of the *CDKN1B* gene encoding p27 are rare. p27 can be functionally disrupted in cancers by excess proteolysis, by decreased translation, or by C-terminal phosphorylation (4, 5).

The phosphatidylinositol 3′-kinase (PI3K) pathway is activated in most human cancers (6) by genetic changes activating receptor tyrosine kinases, PI3K components, or effector kinases (7) or by loss of its negative regulator, phosphatase and tensin homolog (8). PI3K-activated kinases phosphorylate p27 at two sites, T157 and T198. Phosphorylation at T157 in the p27 nuclear localization signal delays nuclear import (9), and T198 phosphorylation stabilizes the protein (10, 11), leading to accumulation of p27 in the cytoplasm. Notably, up to 60% of newly diagnosed breast cancers express activated pAKT, and this correlates with detection of both nuclear and cytoplasmic p27 (9) and with detection of p27pT198 (12) by immunohistochemical analysis. Despite strong cytoplasmic p27 expression, nuclear p27 remains present in all AKT-activated cancers, and cancers with both nuclear and cytoplasmic p27 have a worse prognosis than those with exclusively nuclear p27 (9, 13). Proteomic analysis showed that levels of activated AKTpS473, $p70^{S6K}$pT389, and $p90^{RSK}$pT359 are all strongly correlated with phosphorylated p27pT157 in over 700 primary human breast cancers from The Cancer Genome Atlas (TCGA) and The Cancer Proteome Atlas (TCPA) (14), supporting that PI3K activates p27 phosphorylation in human cancer. It is increasingly clear that p27pT157pT198 drives tumor metastasis via multiple mechanisms. Phosphorylation of p27 at T157 and T198 (9, 15–19) impairs its CDK inhibitory action (20, 21) and promotes binding to RhoA/ROCK1 to disrupt the actin skeleton and enhance cell motility and invasion (18, 22). Increased p27pT157pT198 also facilitates metastases in PI3K-activated cancer models (13, 14) and contributes to epithelial–mesenchymal transformation (EMT) by activating STAT3-dependent TWIST1 induction (14).

p27 is regulated by both the PI3K and TGF-β pathways. Members of the TGF-β family of cytokines bind heterotetrameric TGF-β receptors to activate SMADs, which homo- and heterodimerize and translocate to the nucleus to activate gene expression programs (23, 24). The TGF-β pathway regulates tissue differentiation and morphogenesis in development and activates cytostatic and apoptotic processes to maintain tissue homeostasis (24). Although TGF-β mediates cell cycle arrest via p27 in normal epithelial cells (1, 2), these cytostatic effects are disrupted in cancers, and aberrant TGF-β signaling stimulates EMT, invasion, and metastasis (23, 24). The PI3K and TGF-β pathways have been shown to cooperate to mediate EMT (7), but mechanisms underlying this are not fully known.

The present work reveals a previously unknown mechanism whereby oncogenic activation of the PI3K and TGF-β pathways cooperates to drive EMT and metastasis. We identify a role for

Significance

PI3K is activated in over 60% of human cancers, mediating C-terminal p27 phosphorylation. This work reveals cooperation between PI3K and cJun pathways: p27 phosphorylation by PI3K-activated kinases stimulates p27/cJun corecruitment to chromatin and activation of transcription programs of cell adhesion, motility, *TGFB2*, and epithelial–mesenchymal transformation to drive tumor progression. Prior analysis showed that high p27pT157 strongly associates with activated AKTpS273 and $p90^{RSK}$pT359 in human breast cancers. These cancers also differentially express p27/cJun target genes and identify a poor prognostic group. In cancers, the cell cycle-restraining effects of p27 are lost through increased proteolysis and decreased translation. We reveal a previously unknown oncogenic action of p27, in which p27 acts as a cJun coactivator to drive oncogenic gene expression programs.

Author contributions: H.Y., M.K., K.J., A.B., S.A.W., K.B., L.M., and J.M.S. designed research; J.M.S. obtained grant funding; H.Y., M.K., K.J., A.B., S.A.W., and K.B. performed research; K.J., M.S., and D.Z. contributed new reagents/analytic tools; H.Y., M.K., K.J., M.S., A.B., X.X., S.A.W., L.M., A.M., and J.M.S. analyzed data; and H.Y., M.K., and J.M.S. wrote the paper.

The authors declare no conflict of interest.

This article is a PNAS Direct Submission.

Data deposition: The data reported in this paper have been deposited in the National Center for Biotechnology Information Gene Expression Omnibus database, https://www.ncbi.nlm.nih.gov/geo (accession no. GSE112446).

[1]H.Y. and M.K. contributed equally to this work.

[2]To whom correspondence should be addressed. Email: jslingerland@med.miami.edu.

This article contains supporting information online at www.pnas.org/lookup/suppl/doi:10.1073/pnas.1817415116/-/DCSupplemental.

Published online March 15, 2019.

p27 in which it functionally interacts with cJun as a transcriptional coregulator. p27 and cJun interaction, nuclear localization, and the distribution and extent of p27 and cJun recruitment to chromatin are increased by C-terminal p27 phosphorylation. At a large subset of target genes, cJun binding is p27 dependent, suggesting that p27 may be an obligate cJun coactivator at these sites. *TGFB2* is identified as a p27/cJun target gene required for p27-driven metastasis in vivo. p27/cJun complexes activate oncogenic target gene programs associated with EMT and cancer metastasis, and these target genes are preferentially expressed in primary human breast cancers with high levels of activated p27pT157.

Results

p27 Drives an EMT Gene Expression Program. Prior work showed that C-terminal p27 phosphorylation mediates activation of TWIST1 to drive a morphologic EMT (14). To investigate effects of p27 on metastatic gene programs more broadly, global gene expression assayed by RNA sequencing (RNA-seq) was compared in MDA-MB-231 (hereafter 231), a breast cancer line with low metastatic ability; in MDA-MB-231-1833, a bone-tropic highly metastatic derivative line (25) (hereafter 1833); and in 1833shp27, in which p27 was stably depleted (13). To test the effects of phosphorylated p27pT157pT198, we used 231 transduced with p27 bearing phosphomimetic threonine-to-aspartic acid mutations at T157 and T198 (14). Since as little as two- to threefold p27 overexpression arrests the cell cycle and would not permit study of phosphomimetic p27, p27 was also mutated to p27CK− to abolish cyclin-CDK binding (26), yielding p27CK−DD (14). Notably, comparison of 231 transduced with either p27CK− or p27CK−DD showed only the phosphomimetic p27CK−DD induces a morphologic EMT and confers excess metastasis, indicating that these phosphorylations are critical to p27-driven EMT (14).

Gene ontogeny (GO) analysis revealed activation of programs associated with cell motility, migration, and extracellular matrix (ECM) organization in 231p27CK−DD compared with 231, and in 1833 vs. 1833shp27 (Fig. 1*A*). Differentially expressed genes in these lines were compared with an established "EMT core signature" derived by overexpression of master EMT regulators in human mammary epithelial cells (27). Gene set enrichment analysis (GSEA) showed that genes up-regulated in this signature were increased in 231p27CK−DD compared with 231 and in highly metastatic 1833 vs. 1833shp27, while genes down-regulated in the EMT signature were also decreased in the highly metastatic lines (Fig. 1*B* and *SI Appendix*, Fig. S1*A*). EMT core signature genes differentially expressed in both 231p27CK−DD vs. 231 and 1833 vs. 1833shp27 are shown in Fig. 1*C*. Genes down-regulated during EMT were decreased in 231p27CK−DD and in 1833 compared with both 231 and 1833shp27, while genes activated in the EMT signature were increased in both highly metastatic lines (Fig. 1*C*; see gene list in *SI Appendix*, Table S1). Thus, p27 knockdown reverses the expression of an EMT gene profile, supporting the notion that p27 drives metastasis, in part, by activating an EMT transcription program.

Comparison of EMT markers and drivers showed that 1833 expressed negligible E-Cadherin and Vimentin compared to 231 (Fig. 1*D*). p27-mediated EMT activation was validated by qPCR of major EMT-driving transcription factors in two different breast and bladder cancer models with sister lines of low and high metastatic ability. MDA-MB-231-4175 (hereafter 4175) is a highly metastatic 231 variant with tropism to lung (28), while 1833, as noted above, has bone metastatic tropism (25). UMUC3-LuL2 (hereafter LuL2) is a lung metastatic derivative of the bladder carcinoma line UMUC3 (29). Both metastatic variants have higher PI3K activation and higher p27pT157 and p27pT198 than parental cells (13, 14). p27 depletion decreased expression of the master EMT transcription factors (EMT-TFs) *SNAI1*, *SNAI2*, and *ZEB2* in highly metastatic 1833 and LuL2 (Fig. 1*E*), confirming findings on RNA-seq (*SI Appendix*, Fig. S1*B*), while p27CK−DD transduction up-regulated EMT-TFs in both breast (231) and bladder (UMUC3) lines (Fig. 1*F*).

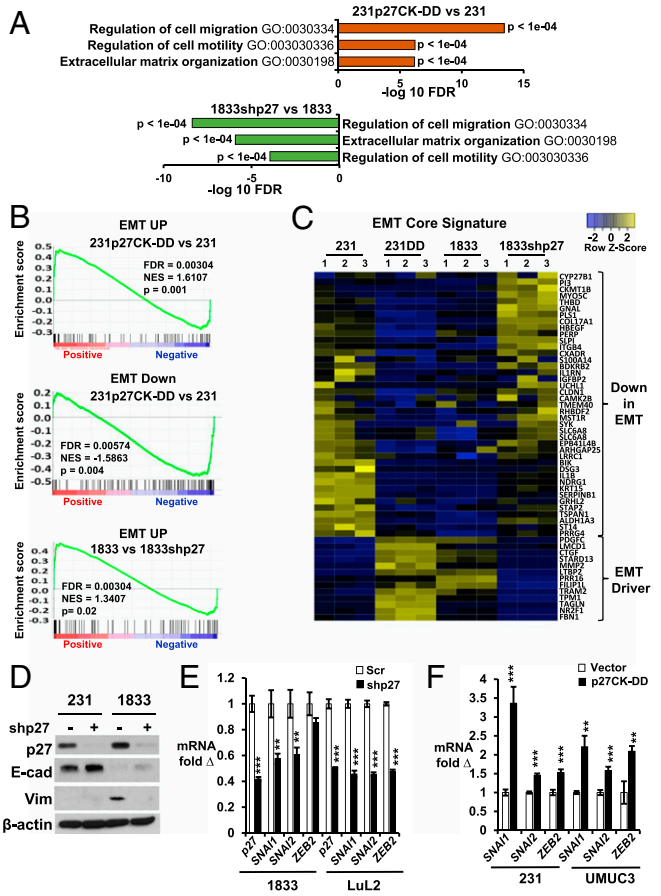

Fig. 1. p27 activates an EMT gene expression program. (*A*) GO analysis of genes governing cell migration, motility, and ECM in 231 vs. 231p27CK−DD and in 1833 vs. 1833shp27. FDR, fold discovery rate. (*B*) GSEA shows differential expression of EMT core signature genes (27) up-regulated (EMT UP) and down-regulated (EMT Down) in the indicated lines. Normalized enrichment score (NES), FDR, and *P* values are shown. (*C*) Heatmap of mean fold changes in differentially expressed EMT core signature genes in parental 231, 231p27CK−DD, 1833, and 1833shp27. Genes altered by p27 knockdown revert away from the Taube et al. (27) EMT core signature. Genes are listed in *SI Appendix*, Table S1. (*D*) Effects of stable p27 depletion in 1833 on p27 and the EMT markers E-cadherin (E-cad) and Vimentin (Vim) by Western blot (β-actin as loading control; data representative of more than three repeat assays). (*E*) Effects of stable p27 depletion (shp27) on qPCR expression of EMT-TFs (*SNAI1*, *SNAI2*, and *ZEB2*) in PI3K-activated lines (1833 and LuL2) vs. scramble shRNA controls (Scr). (*F*) Effects of stable p27CK−DD expression on expression of EMT-TFs in 231 and UMUC3 vs. vector-only control lines. In *E* and *F*, means ± SEM graphed from three or more replicates of three or more biologic assays (***P* < 0.01, ****P* < 0.001). 231DD, 231p27CK−DD. See also *SI Appendix*, Fig. S1 *A* and *B*.

p27pT157pT198 Activates TGF-β Signaling by Inducing *TGB2* Expression. To further identify p27-regulated gene programs, we focused on genes both stringently up-regulated by p27CK−DD transduction in 231 and down-regulated in 1833 by p27 depletion. A total of 489 genes were increased by over twofold ($P < 0.005$, $q < 0.1$) in 231p27CK−DD vs. 231, while 229 genes were down-regulated by at least one half (fold change > 0.5, $P < 0.005$, $q < 0.1$) by p27 depletion in 1833. Of these, 82 genes were both up-regulated in 231p27CK−DD vs. 231 and also down-regulated in 1833shp27 vs. 1833 (Fig. 2*A* and *SI Appendix*, Table S2). GO analysis showed that the 82 genes that are both up-regulated by p27CK−DD in 231 and down-regulated in 1833 upon p27 loss are associated with important oncogenic pathways, including TGF-β, focal adhesion, ECM receptor interaction, and PI3K-AKT signaling pathways (Fig. 2*B* and *SI Appendix*, Fig. S1*C*). GSEA also showed TGF-β signaling

activation in 231p27CK–DD compared with 231, while p27 knockdown impaired TGF-β pathway activation in 1833 (Fig. 2 *C* and *D* and *SI Appendix*, Fig. S1*D* and Table S3). Similarly, treatment with the PI3K/mammalian target of rapamycin (mTOR) inhibitor, PF04691502 (hereafter PF1502), at a dose known to inhibit PI3K in these lines and to decrease both p27pT157 and p27pT198 (13), down-regulated genes associated with TGF-β pathway activation (*SI Appendix*, Fig. S1 *D* and *E*). Thus, TGF-β signaling is activated by p27CK–DD transduction in 231 and inhibited by p27 knockdown and by PI3K inhibition in 1833.

Up-regulation of *TGFB2* by p27 was confirmed by qPCR in three highly metastatic lines: 1833, 4175, and LuL2. In all three lines, p27 depletion decreased *TGFB2* expression (Fig. 2*E*). Furthermore, p27CK–DD transduction increased *TGFB2* expression and TGF-β2 secretion in the immortal, nontransformed mammary epithelial line MCF12A and in the low-metastatic 231 and UMUC3 lines (Fig. 2 *F* and *G*). In MCF12A, TGF-β2 induced a morphological change from an epithelial to a more mesenchymal phenotype (*SI Appendix*, Fig. S1*F*). TGF-β2 up-regulated *SNAI1* and *SNAI2* expression in MCF12A, 231, and UMUC3 (*SI Appendix*, Fig. S1*G*) and increased Matrigel invasion by 231 and UMUC3 (Fig. 2*G* and *SI Appendix*, Fig. S1*H*), confirming its importance to EMT in these models. In 231, EMT activation by p27CK–DD was shown by increased Matrigel invasion, decreased E-cadherin, and higher EMT-TF expression. All of these were reversed by *TGFB2* depletion (Fig. 2 *H–J*), indicating that TGF-β2 is a key driver of EMT activation by p27. Thus, C-terminally phosphorylated p27 appears to activate an EMT program, in part, by inducing *TGFB2* expression.

p27/cJun Complex Formation and Nuclear Localization Are Regulated by p27 Phosphorylation. To investigate how p27 up-regulates *TGFB2* expression, a phosphoprotein array was compared in MCF12A and MCF12Ap27CK–DD. Notably, p27CK–DD expression significantly increased serine 63-phosphorylated, activated cJun (hereafter cJunpS63) in MCF12A (Fig. 3*A*). p27CK–DD–transduced 231 and UMUC3 also had more cJunpS63 than parental lines, while p27 depletion in metastatic 1833 and LuL2 lines decreased cJunpS63 (Fig. 3*B*). cJun forms heterodimeric AP-1 transcription factor complexes that contribute to transformation (30). An in silico search revealed AP-1 consensus binding sites upstream of the *TGFB2* coding sequence.

To test whether p27 might interact with cJun to regulate *TGFB2* expression, we next assayed if cellular p27 binds cJun. Treatment of LuL2 with PF1502 over 48 h decreased AKTpS473 and reduced p27 phosphorylation at T198 (Fig. 3*C*, *Left*) without affecting p27 or cJun levels. cJun was detected in cellular p27 immunoprecipitates in LuL2. PI3K inhibition decreased both p27pT198 and p27-bound cJun (Fig. 3*C*). Furthermore, more p27-associated

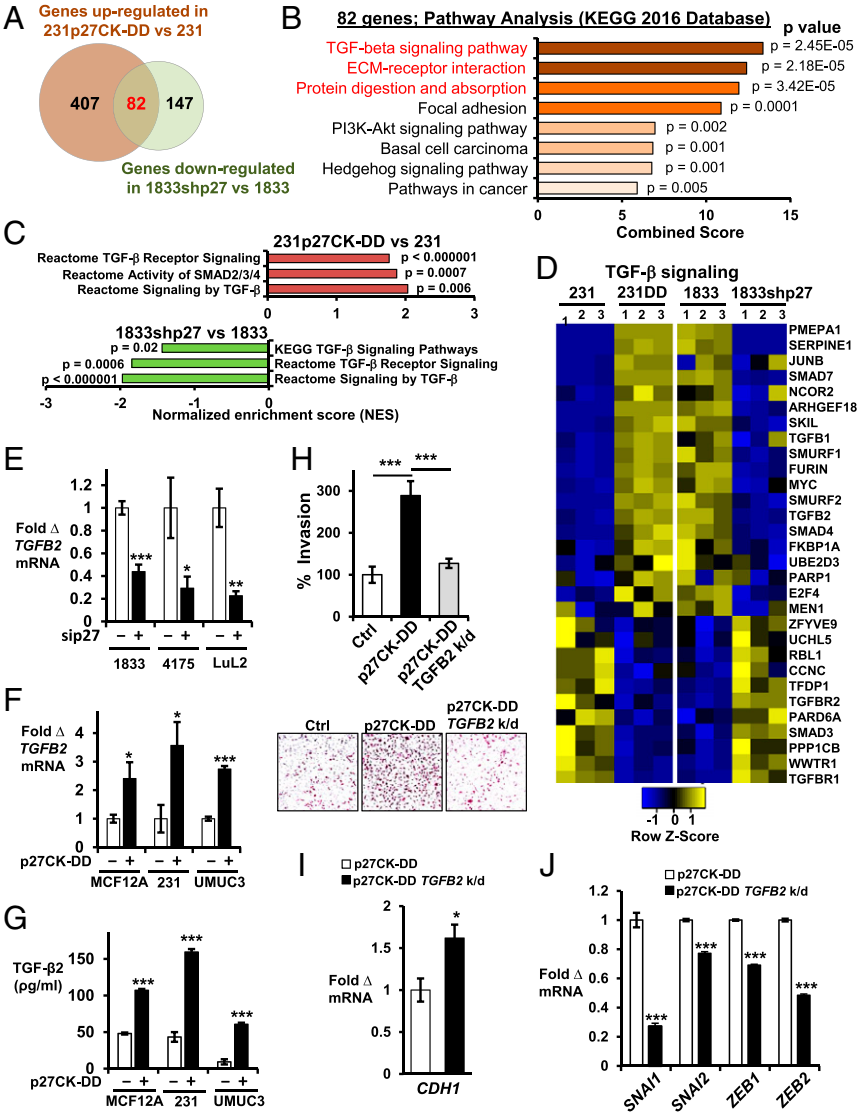

Fig. 2. TGF-β signaling is regulated by p27. (*A*) Venn diagram depicts genes up-regulated in 231p27CK–DD vs. 231 (fold change >2.0, $P < 0.005$, $q < 0.1$) and down-regulated in 1833shp27 vs. 1833 (fold change <0.5, $P < 0.005$, $q < 0.1$). Numbers of genes are indicated. See also *SI Appendix*, Table S2. (*B*) GO analysis shows the top signaling pathways in the Kyoto Encyclopedia of Genes and Genomes (KEGG) 2016 database related to the 82 genes up-regulated in 231p27CK–DD vs. 231 and that decreased with p27 loss in 1833. See also *SI Appendix*, Fig. S1*C*. (*C*) Pathway analysis of these 82 differentially expressed genes. NES, normalized enrichment score. See also *SI Appendix*, Fig. S1*D*. (*D*) Heatmaps show differential expression of 30 TGF-β signaling pathway genes from three independent RNA-seq experiments. See also *SI Appendix*, Fig. S1 *D* and *E* and Table S3. (*E*) Effects of short-term siRNA-mediated p27 depletion (sip27) on *TGFB2* mRNA by qPCR at 48 h in PI3K-activated, metastatic lines (1833, 4175, and LuL2) vs. scramble siRNA controls. (*F* and *G*) Effects of stable p27CK–DD expression on *TGFB2* mRNA (*F*) and on secreted TGF-β2 (pg/mL) over 48 h (*G*) in the indicated lines. (*H*) Quantitative data (*Top*) and representative images (*Bottom*) of Matrigel invasion in 231, 231p27CK–DD, and *TGFB2*-depleted (*TGFB2* k/d) 231p27CK–DD (for *TGFB2* depletion, see *SI Appendix*, Fig. S4*A*). (*I* and *J*) Effects of *TGFB2* depletion on *CDH1* expression (*I*) and on EMT drivers (*SNAI1*, *SNAI2*, *ZEB1*, and *ZEB2*) (*J*). Means ± SEM graphed from three or more replicates of three or more different biologic assays (*$P < 0.05$, **$P < 0.01$, ***$P < 0.001$). 231DD, 231p27CK–DD. See also *SI Appendix*, Fig. S1 *F–H*.

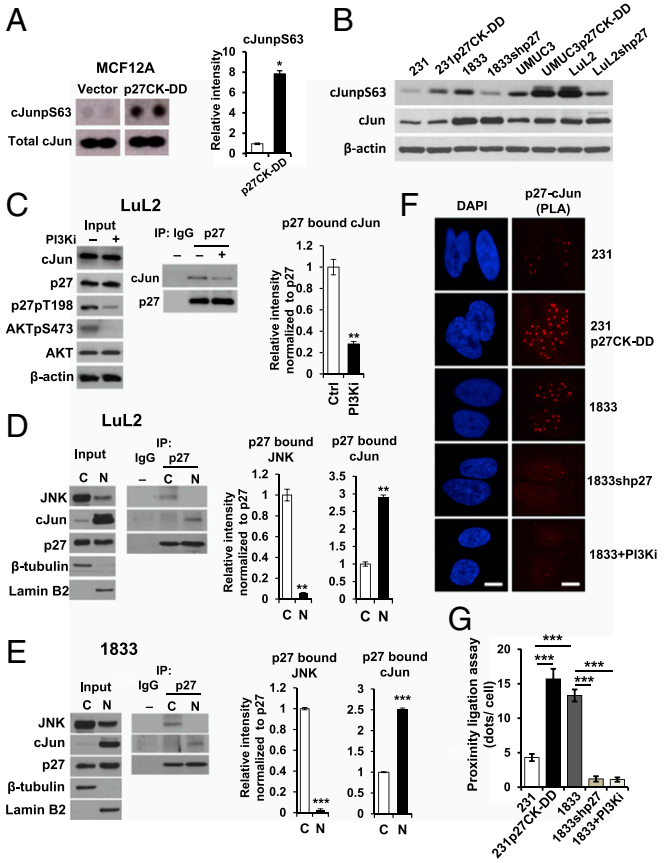

Fig. 3. Association of cJun with p27 is increased by p27 phosphorylation. (*A*) Activated cJun (cJunpS63) in MCF12A controls (Vector) and MCF12Ap27CK−DD (p27CK−DD) by dot blot (*Left*) and densitometry values graphed as mean ± SEM (*Right*, $*P < 0.05$). (*B*) Western blots of cJun, cJunpS63, and β-actin in the indicated lines. (*C*) LuL2 treated for 48 h with the PI3K inhibitor PF1502 (PI3Ki). Western blots show input (*Left*) for p27 immunoprecipitation (IP) blotting to detect p27-associated cJun (*Middle*). Densitometric quantitation of p27-bound cJun (*Right*, $**P < 0.01$). See also *SI Appendix*, Fig. S2 *A* and *B*. (*D* and *E*) Nuclear (N) and cytoplasmic (C) fractions of LuL2 (*D*) and 1833 (*E*) were immunoblotted (*Left*), and p27-associated cJun and JNK were detected by IP blot (*Middle*) with densitometry (*Right*, $**P < 0.01$, $***P < 0.001$). (*F*) In situ PLA shows p27/cJun complexes in the indicated lines and in 1833 treated with PF1502 (PI3Ki), indicated by red fluorescent dots. (*G*) Dots (mean ± SEM) graphed from triplicate PLAs; ANOVA with post hoc comparisons ($***P < 0.001$). (Scale bar: 10 μm.) See also EMSA data in *SI Appendix*, Fig. S2C.

cJun was detected in p27CK−DD–transduced 231 and UMUC3 than in vector control cells, as assayed by densitometry (*SI Appendix*, Fig. S2 *A* and *B*). These observations suggest that the interaction of p27 with cJun is increased by p27 phosphorylation.

Levels of p27-associated cJun and Jun N-terminal kinase (JNK) were assessed in nuclear and cytoplasmic fractions. In both LuL2 and 1833, JNK was largely cytoplasmic, while cJun was predominantly nuclear (Fig. 3 *D* and *E*, *Left*). p27-associated cJun was two- to threefold higher in nuclear vs. cytoplasmic fractions, while p27-associated JNK was detected only in the cytoplasm (Fig. 3 *D* and *E*, *Right*). Proximity ligation assays (PLAs) confirmed the interaction between nuclear p27 and cJun and that this interaction is greater in 231p27CK−DD than in control 231 cells (Fig. 3 *F* and *G*). Electrophoretic mobility shift assay (EMSA) revealed that p27 can bind an AP-1 consensus motif (*SI Appendix*, Fig. S2C).

cJun and p27 Are Corecruited to a Site Upstream of *TGFB2*. Since p27 could associate with cJun and bind to AP-1 motifs, we next assayed if nuclear p27/cJun complexes might mediate the *TGFB2* gene induction observed in p27-activated cells. Publicly available cJun ChIP sequencing (ChIP-seq) ENCODE data revealed that cJun binds a 5′-TGAG/CTCA-3′ AP-1 consensus site upstream of the *TGFB2* transcriptional start site (TSS) in human cells (Fig. 4*A*). ChIP-qPCR showed that cJun and p27 are corecruited to this AP-1 site. More p27 and cJun were associated with this AP-1 motif in 231p27CK−DD and 1833 than in 231 vector controls. Notably, chromatin association of both p27 and cJun decreased with p27 depletion and with loss of p27 phosphorylation following PI3K/mTOR inhibition with PF1502 (Fig. 4 *B* and *C*). Neither p27 nor cJun bound to irrelevant sites (*SI Appendix*, Fig. S3*A*). Sequential ChIP assays with cJun followed by re-ChIP with p27 antibodies indicated that cJun and p27 co-occupy this *TGFB2* site, with greater recruitment in p27CK−DD–expressing and PI3K-activated cells, and with loss of both p27 and cJun from this site upon p27 knockdown and PI3K inhibition (Fig. 4*D*). Thus, C-terminal p27 phosphorylation appears to increase cJun/p27 corecruitment to this AP-1 motif upstream of *TGFB2*. The bladder cancer models showed similar patterns of p27 and cJun recruitment to this *TGFB2* AP-1 site (*SI Appendix*, Fig. S3*B*). H3K27Ac, coactivator CBP/p300, and RNA polymerase II (Pol II) were more abundant at this *TGFB2* site in p27pT157pT198 or p27CK−DD–expressing cells than in 231 controls and decreased significantly with p27 depletion and PI3K inhibition in 1833 (Fig. 4 *E*–*G*). Because p27 knockdown decreases *TGFB2* expression and because p27CK−DD transduction induces *TGFB2*

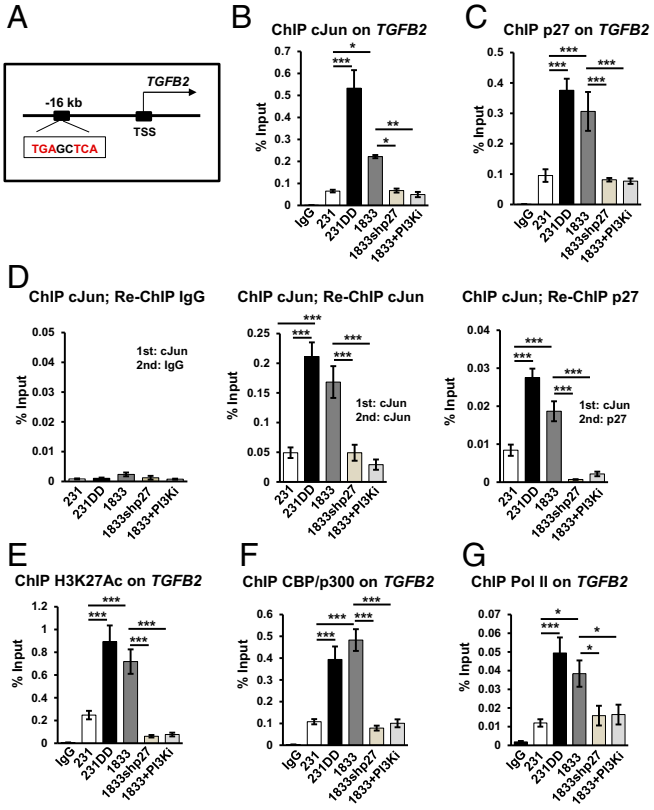

Fig. 4. cJun and p27 are corecruited to a *TGFB2* AP-1 site. (*A*) cJun/AP-1 consensus motif upstream of *TGFB2* TSS. (*B* and *C*) ChIP-qPCR with cJun (*B*) and p27 (*C*) antibodies show binding to an AP-1 site upstream of *TGFB2* in the indicated lines and in 1833 treated for 48 h with PF1502 (PI3Ki). (*D*) ChIP-re-ChIP assay of p27 association with cJun-bound *TGFB2* AP-1 site in the indicated lines. (*E*–*G*) ChIP assays show H3K27Ac (*E*), CBP/p300 (*F*), and Pol II (*G*) binding to the *TGFB2* AP-1 site in the indicated lines. Means ± SEM graphed from three or more replicates of three or more biologic assays; post hoc *P* values from ANOVA ($*P < 0.05$, $**P < 0.01$, $***P < 0.001$). See also *SI Appendix*, Fig. S3. 231DD, 231p27CK−DD.

to increase TGF-β2 secretion, these data suggest a model in which C-terminal p27 phosphorylation promotes p27 and cJun recruitment as well as interaction with CBP/p300 and Pol II at this enhancer to induce *TGFB2* expression (*SI Appendix*, Fig. S3*C*).

cJun and TGF-β2 Mediate p27-Driven Metastasis from Primary Tumors in Vivo. Since p27 appears to drive a TGF-β2–dependent EMT, we assayed the functional contribution of C-terminally phosphorylated p27, cJun, and TGF-β2 to metastasis in vivo. NOD-SCID mice were injected orthotopically with 231, 1833, 1833shp27, and 231p27CK−DD, and with 231p27CK−DD depleted of either *JUN* or *TGFB2* (depletion shown in *SI Appendix*, Fig. S4*A*). After removal of primary tumors at 300 mm^3, mice were monitored for metastasis from the primary site. Orthotopic injection of each of 1833 and 231p27CK−DD yielded significantly more metastases in liver, lymph nodes, and lung than vector control 231 cells (Fig. 5 *A*–*C*). p27 depletion in 1833 and loss of cJun or TGF-β2 expression in 231p27CK−DD significantly decreased p27-driven metastasis in vivo (Fig. 5 *A*–*C*). While 1833 and 231p27CK−DD formed more metastasis than 231, primary tumor growth and Ki67 staining did not differ significantly between groups (*SI Appendix*, Fig. S4 *B* and *C*). TGF-β2 levels, assayed by immunohistochemistry, were elevated in primary tumors from 1833 and 231p27CK−DD compared with 231 and were decreased in 1833shp27 tumors and in both *JUN*- and *TGFB2*-depleted 231p27CK−DD–derived tumors (Fig. 5*D* and *SI Appendix*, Fig. S4*D*). Thus, cJun activation and *TGFB2* induction appear to be required for p27-driven metastasis in this breast cancer model.

Identification of cJun/p27-Regulated Target Genes. To test if p27 binds more broadly to chromatin and to identify phosphorylation-dependent patterns of chromatin occupancy by p27 and cJun, ChIP-seq was performed in 231, 231p27CK−DD, and 1833. As a control, we also performed p27 ChIP-seq in 1833shp27. This revealed that p27 is broadly recruited to chromatin and that a significant proportion of cJun ChIP-seq peaks also contain p27 (Fig. 6*A*), suggesting that cJun and p27 may function together at common sites. Notably, 231p27CK−DD showed greater recruitment not only of p27 but also of cJun to chromatin, even at sites not shared by p27. The latter may result from p27-mediated cJun activation (Fig. 3*B*). Genomic distribution analysis showed that a little over half of the sites bound by cJun, p27, and both cJun/p27 are located at promoters or intronic sites, whereas the remaining sites occupy intergenic regions (Fig. 6*B*). Importantly, ChIP-seq heatmaps showed that the p27 signal was abrogated in p27-depleted 1833shp27 cells (Fig. 6*C*). Interestingly, the chromatin occupancy of cJun was also modulated by p27 depletion: among a

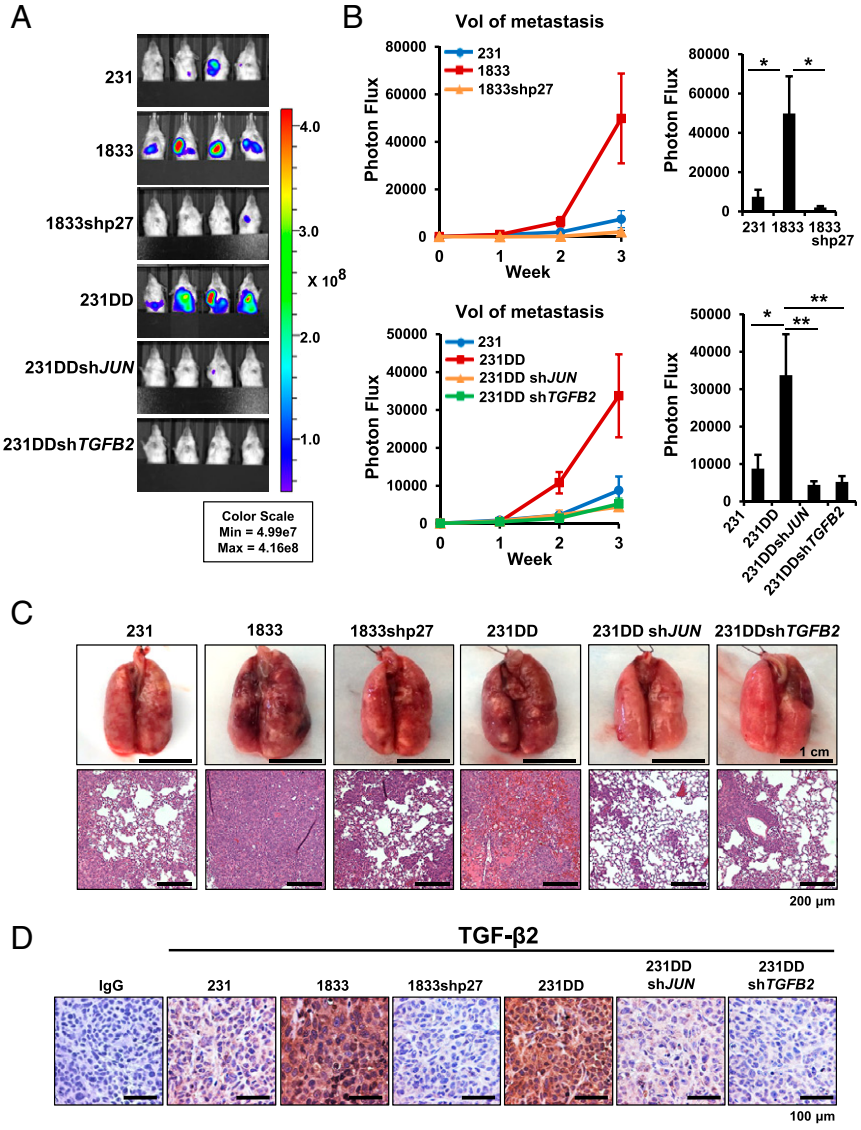

Fig. 5. cJun and TGF-β2 are required for p27-driven metastasis in vivo. (*A*) Primary orthotopic tumors were removed and animals were followed for metastasis using the bioluminescence in vivo imaging system (IVIS). Representative bioluminescence images of tumor-bearing mice 3 wk after primary tumor removal. Color scale depicts photon flux (photons per second) from tumor-bearing mice. (*B*) Mean (±SEM) bioluminescence (normalized photon flux) per second from tumor metastases (excluding regrowth of primary tumor at inguinal fat pad) is graphed for each group. *P* values from ANOVA (*$P < 0.05$, **$P < 0.01$, ***$P < 0.001$). (*C*) Representative whole-lung images (scale bar: 1 cm) and photomicrographs (scale bar: 200 μm) of metastatic lung tumors from the indicated groups. (*D*) Representative TGF-β2 immunohistochemistry images in primary tumors from the indicated lines. (Scale bar: 100 μm.) 231DD, 231p27CK−DD. See also *SI Appendix*, Fig. S4.

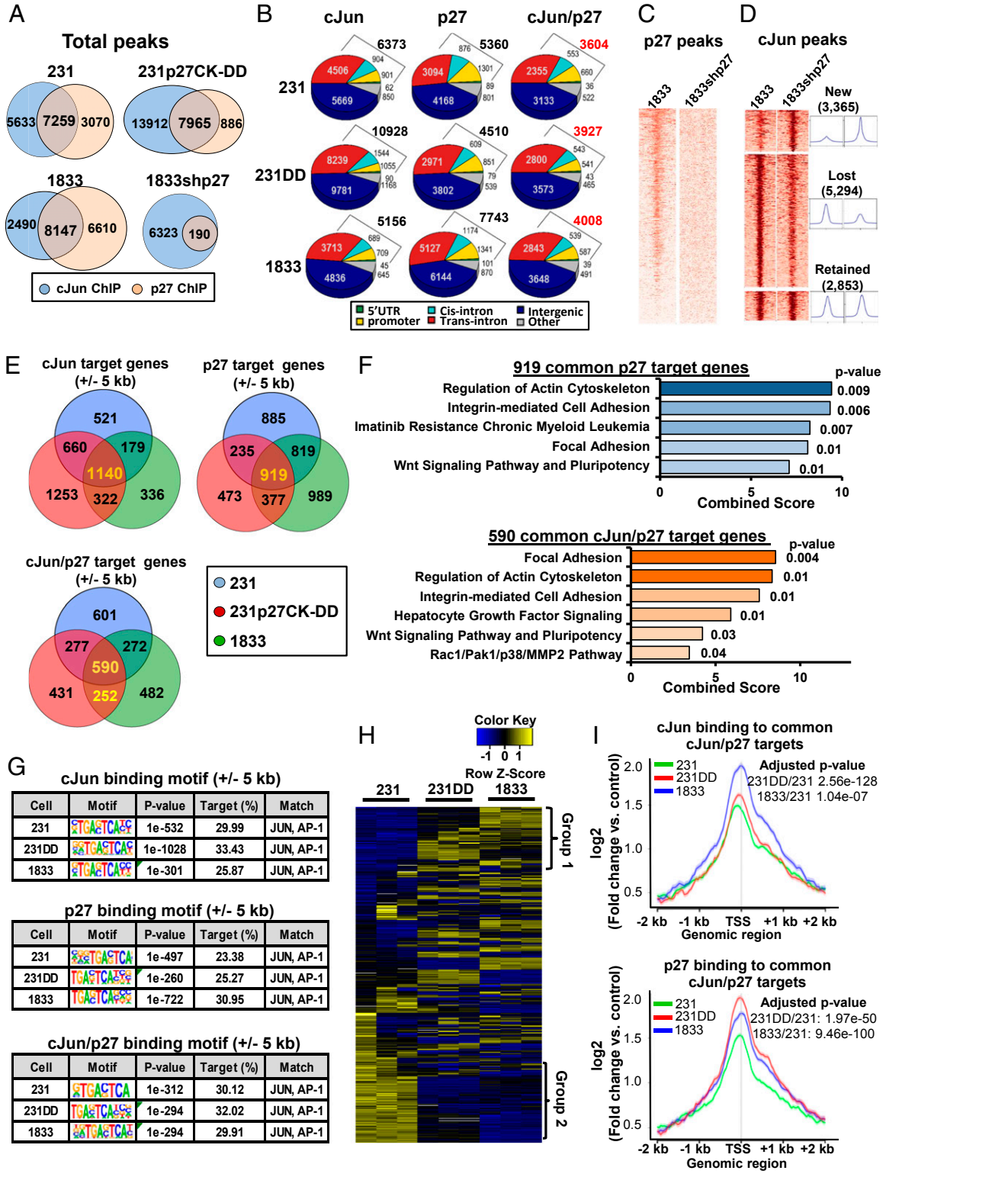

Fig. 6. Genome-wide DNA binding of p27 and cJun. (*A*) Venn diagrams show mean p27- and cJun-DNA binding peaks in 231, 231p27CK–DD, 1833, and 1833shp27 from two independent ChIP-seq assays, each with two biologic replicates. (*B*) Genomic distribution of DNA binding peaks for p27, cJun, and for peaks occupied by both p27 and cJun in the indicated lines. (*C* and *D*) DNA binding heatmaps of p27 (*C*) and cJun ChIP (*D*) in 1833 and 1833shp27. See also *SI Appendix*, Fig. S5*A* and see *SI Appendix*, Fig. S5*B* for cJun-regulated pathways affected by loss of p27. (*E*) Venn diagrams show mean numbers of target genes (±5 kb from the TSS) bound by cJun only, p27 only, and both cJun and p27 in 231, 231p27CK–DD, and 1833. (*F*) GO analysis (WikiPathway 2016) showing major signaling pathways related to 919 p27 target genes and 590 cJun/p27 cotarget genes bound in all three lines from *E*. See also *SI Appendix*, Fig. S5*C*. (*G*) Binding motif search shows top transcription motif bound by cJun only, p27 only, and cJun/p27 for binding motifs ±5 kb from the TSS for each line. See *SI Appendix*, Fig. S5*D* for binding at all sites. (*H*) Heatmaps show expression profile from RNA-seq of genes bound by both cJun and p27 in ChIP-seq in all three lines. (*I*) Signal intensities of p27 and cJun were quantitated at target genes bound by both cJun and p27 in all three cell lines. Significant differences calculated with paired *t* test, and *P* values adjusted by Bonferroni–Hochberg. See also *SI Appendix*, Fig. S5 *E* and *F* and Table S4 for signal intensities of cJun and p27 binding to group 1 and group 2 genes, respectively. 231DD, 231p27CK–DD.

little over 10,000 cJun-bound peaks detected in 1833, 5,294 sites were shared by p27 and were lost or decreased upon p27 knockdown, while 2,853 cJun-bound peaks were unaffected. In addition, 3,365 new, exclusively cJun-bound peaks were acquired (Fig. 6*D* and *SI Appendix*, Fig. S5*A*). GO analysis of 1,364 genes annotated by the 5,294 cJun-bound peaks that are lost with p27 depletion in 1833 showed that these p27-regulated cJun targets are associated with Notch, apoptosis, and cytoskeleton signaling (*SI Appendix*, Fig. S5*B*). Thus, p27 may be required for cJun recruitment to an important fraction of cJun-regulated genes.

Evaluation of binding at target genes (±5 kb from the TSS) revealed that p27 is recruited to over 2,000 target genes in each of the three lines (Fig. 6*E*, *Top Right* Venn diagram). Notably, GO analysis of the 919 p27 targets common to all three lines reveals that p27 binds genes involved in focal adhesion, actin cytoskeleton, integrin signaling, and Wnt pathways (Fig. 6*F*, *Top*). GO analysis of cJun targets common to all three lines identifies genes governing cell surface adhesion, integrin and growth factor pathways (*SI Appendix*, Fig. S5*C*). There were 590 cJun/p27 target genes commonly bound in all three lines (Fig. 6*E*, *Bottom* and *SI Appendix*, Table S4). These are associated with pathways similar to those for each factor alone and also include hepatocyte growth factor and Rac1/Pak1 signaling (Fig. 6*F*, *Bottom*). p27 and cJun were also corecruited to 252 novel target genes in both 231p27CK−DD and 1833 that were not bound in 231 (Fig. 6*E*, *Bottom*).

DNA binding motif analysis revealed that AP-1 binding consensus motifs, including JunB, Fra1, and BATF, were the top-enriched DNA motifs for p27 and cJun individually and account for nearly one-third of the sites bound by both cJun and p27 (binding motifs ±5 kb from the TSS, Fig. 6*G*; genome-wide binding motifs in *SI Appendix*, Fig. S5*D*). Thus, p27 and cJun are commonly recruited to genes bearing cJun consensus motifs.

Differential Expression of cJun/p27 Target Genes in Lines with Different Metastatic Potential. To evaluate the potential for p27 and cJun to coregulate gene expression, patterns of chromatin annotation were compared with RNA-seq gene expression data. Of the 919 genes annotated by p27 in all three lines, over half were differentially expressed in 231p27CK−DD (492/919) and in 1833 (456/919) compared with 231 (any fold change vs. 231, q > 0.1). cJun/p27 target genes bound in all three lines showed two differential expression patterns. Group 1 genes were up-regulated in 231p27CK−DD and in 1833 compared with 231 controls, while group 2 genes were down-regulated. cJun/p27 target genes activated in both highly metastatic lines identify putative oncogenes (group 1, Fig. 6*H*), while those down-regulated in metastatic derivatives compared with control 231 may encode tumor suppressors (group 2, Fig. 6*H*).

Lines with p27 activation showed greater recruitment of both cJun and p27 to target genes: recruitment of both p27 and cJun to all 590 common target genes (Fig. 6*I*) and to differentially expressed cJun/p27 targets from both groups 1 and 2 (*SI Appendix*, Fig. S5 *E* and *F*) was significantly greater in 231p27CK−DD and 1833 than in 231, similar to the pattern detected at the *TGFB2* AP-1 site (Fig. 4). Differential expression of cJun/p27-activated group 1 genes and p27 and cJun binding intensities are shown in Fig. 7 *A* and *B* and *SI Appendix*, Table S4. These cJun/p27-activated genes associated strongly with cancer signaling pathways, including prooncogenic p53, cancer-related miRNAs, focal adhesion, the receptor for advanced glycation end- products (RAGE), and hypoxia inducible factor-1 (HIF-1) (Fig. 7*C*).

cJun/p27 targets that were bound exclusively in 1833 and 231p27CK−DD, but not in 231, might include novel prooncogenes whose binding is only acquired when highly phosphorylated p27pT157pT198 binds cJun. A subset of these novel cJun/p27 target genes was up-regulated in the highly metastatic lines (Fig. 7 *D* and *E* and *SI Appendix*, Table S5). This gene set also directs pathways associated with tumor progression and metastasis (Fig. 7*F*). We validated p27 and cJun binding to three target genes (*MYO10*, *PAI1*, and *KLF8*) by ChIP-qPCR and verified their differential expression by RT-qPCR. *MYO10* is a gene implicated in cell invasion and metastasis (31). Both the binding of cJun and p27 to an AP-1 site +2 kb from *MYO10* and *MYO10* expression were greater in 231p27CK−DD and 1833 than in 231 and were down-regulated in 1833shp27 (*SI Appendix*, Fig. S6 *A–D*). Differential cJun/p27 binding to, and induction of, two other target genes, *PAI1*/*SERPINE1* [a known prognostic factor for breast cancer (32)] and *KLF8* [an EMT mediator (33)], were also verified (*SI Appendix*, Fig. S6 *E–L*). Together, p27 appears to bind cJun and promote recruitment to, and transactivation of, gene programs that contribute to tumor progression and metastasis.

p27/cJun Target Genes Are Differentially Expressed in Breast Cancers with High p27pT157. We next assayed if primary human breast cancers with C-terminally phosphorylated p27 would show differential expression of cJun/p27-regulated genes identified herein. Among primary breast cancers in the TCGA database, 846 had gene expression, p27pT157 levels on reverse phase protein array, and outcome data available. Of these, cancers in the top decile of p27pT157 expression showed significantly worse overall survival (OS) (Fig. 7*G*, $P = 0.028$). A subset of 392 genes, differentially expressed in the "p27pT157 high" breast cancers vs. all others, was also coordinately differentially expressed in p27-activated 231p27CK−DD and 1833 compared with 231 and 1833shp27. Of these 392 differentially expressed genes, 25% (97/392) were Jun-bound and 16% (63/392) showed both p27 and cJun binding on ChIP-seq and included the validated target, *PAI1*. Univariate and multivariate analysis of each of these genes in a training dataset of 702 breast cancers identified the 30 p27-regulated genes differentially expressed both in p27-activated cell lines and in the cancers with high p27pT157 that contribute most importantly to patient outcome. Principle component analysis showed that these 30 genes cluster patients into two groups (Fig. 7*H*) that have significantly different OS on Kaplan–Meier analysis (Fig. 7*I*, $P = 0.036$). The prognostic value of this p27-regulated gene signature for OS was validated using receiver operating characteristic (ROC) curve analysis in an independent breast cancer validation cohort and yielded an area under the ROC curve (AUC) of 0.63 at 5 y and of 0.73 at 6 y of follow-up (Fig. 7*J*). The coordinate expression of p27-regulated gene drivers of poor patient outcome both in p27-activated cancer lines and in primary breast cancers with high C-terminal p27 phosphorylation supports the biologic relevance of p27-driven gene regulation to metastatic tumor progression.

Discussion

The cyclin-CDK inhibitor p27 is a ubiquitously expressed, critical negative regulator of the G1 to S phase cell cycle transition (4). p27 inhibits cyclin-CDK complexes in the nucleus of quiescent cells but accumulates in the cytoplasm in early G1 (34). Transient C-terminal p27 phosphorylation by pAKT in early G1 delays nuclear p27 import (9) and promotes cyclin D-CDK4/6 assembly and activation (21, 35, 36) as Src and cyclin E-Cdk2 phosphorylate p27 to mediate its proteolysis and promote G1 transit (37, 38). The coordinate phosphorylation of p27 at T157 and T198 also promotes its binding to RhoA/ROCK1 (18) to alter the actin cytoskeleton in normal cells, mediating changes in cell shape required for execution of later cell cycle phases (39, 40).

In the last two decades, p27 has been found to act as both tumor suppressor and oncogene and as a critical regulator of development. The present work opens the possibility that these roles might be modulated by a transcriptional regulatory action of p27. p27 deregulation is a hallmark of human cancers. The tumor-suppressor, CDK-inhibitory function of p27 is impaired through miRNA-mediated decreases in p27 translation and by accelerated p27 proteolysis in Src-activated cells (4). p27 also acquires prooncogenic functions through its C-terminal phosphorylation by PI3K-activated kinases (41). C-terminal p27 phosphorylation at T157 and T198 attenuates CDK inhibitory action and increases cyclin D-CDK activation (21, 35) and disrupts the actin cytoskeleton through RhoA/ROCK1 inactivation (18, 22) to promote cancer metastasis (42). Enforced expression of p27 in the cytoplasm of malignant

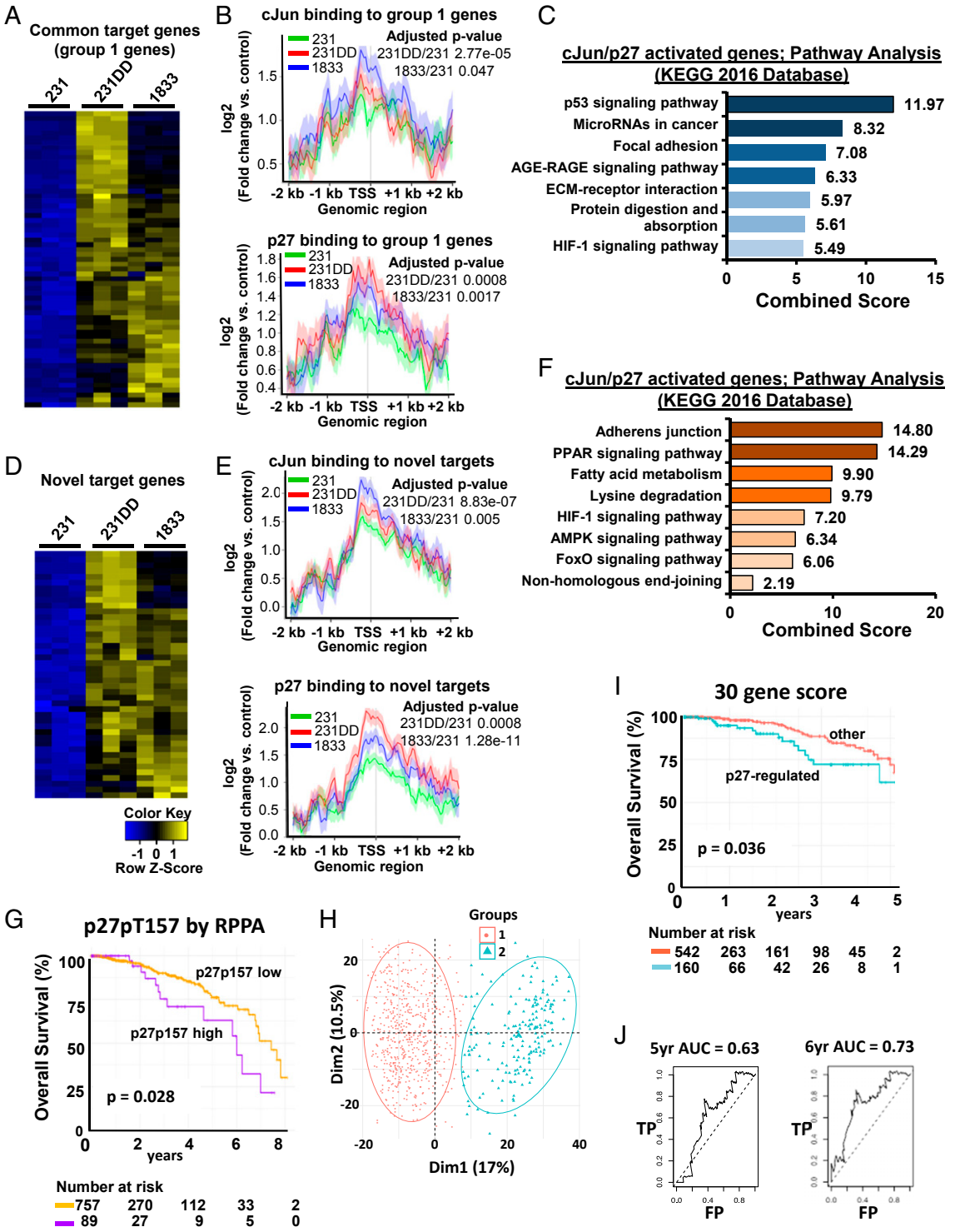

Fig. 7. cJun/p27-regulated target genes govern cancer programs of tumor progression. (*A*) Heatmap of expression of 61 p27/cJun target genes common to all three lines whose expression is up-regulated in 231p27CK–DD (231DD) and 1833 lines vs. 231. See also *SI Appendix*, Table S4. (*B*) Mean amplitudes of target gene binding by cJun (*Top*) and p27 (*Bottom*) are shown for the differentially expressed genes in *A* in the indicated cell lines. (*C*) GO analysis shows the top signaling pathways related to the differentially expressed genes identified in *A*. (*D*) Heatmap of expression of 43 newly acquired cJun/p27 target genes bound in 231DD and 1833, but not in 231, that are differentially expressed in the indicated cell lines. See also *SI Appendix*, Table S5. (*E*) Mean amplitude of target gene binding by cJun (*Top*) and p27 (*Bottom*) are shown for the differentially expressed genes in *D* in the indicated cell lines. (*F*) GO analysis shows the main signaling pathways related to the genes identified in *D*. See *SI Appendix*, Fig. S6 for validation of cJun/p27 cotarget genes. (*G*) Kaplan–Meier (KM) graph showing differential OS among women whose breast cancers have high vs. low p27pT157 on reverse phase protein array (RPPA) from $n = 846$ cases in the TCGA/TCPA dataset. (*H*) Principle component analysis of 30 p27-regulated genes expressed among $n = 703$ breast cancers. (*I*) KM graph shows overall breast cancer survival according to differential expression of the p27-regulated 30 gene profile among the training set ($n = 703$ cases). (*J*) The prognostic value of this p27-regulated 30 gene signature for OS was validated using ROC analysis in an independent breast cancer validation cohort. AGE-RAGE, advanced glycation end products-receptor for advanced glycation end products; AMPK, 5′ AMP-activated protein kinase; FP, false positive; KEGG, Kyoto Encyclopedia of Genes and Genomes; PPAR, peroxisome proliferator-activated receptor; TP, true positive.

cells with high endogenous PI3K activation is sufficient to increase cell invasion and metastasis (43, 44). Although aberrantly detected in cytoplasm, p27 is never exclusively cytoplasmic, nor is nuclear p27 limited in PI3K-activated cancers (9, 15, 16). Delayed nuclear import and increased stability of C-terminally phosphorylated p27 permit novel protein interactions in both cytoplasm and nucleus that drive oncogenesis. Our prior work showed that p27CK−DD, but not p27CK−, interacts with and activates STAT3 to induce *TWIST1* expression and a morphologic EMT and showed that C-terminal p27 phosphorylation critically mediates metastasis (14). Here, we identify a mechanism of oncogene cooperation between the PI3K pathway and cJun and reveal a previously unknown p27/cJun partnership that provides new insight into the profound effects of p27 on tumor metastasis. It is not clear that any of the p27 phenotypes resulting from these phosphorylations has primacy over any other. Rather, we posit that they would act together to promote transformation in the context of constitutive oncogenic PI3K activation. We show that p27 is broadly recruited to chromatin and cooperates with cJun to activate gene programs that govern focal adhesion, cytoskeleton, and signaling regulators of cell motility and metastasis.

Several lines of evidence have suggested a role for p27 in transcriptional regulation during embryogenesis. As CDK inhibitor, p27 acts to coordinate cell cycle exit with terminal differentiation (40, 41). p27 also plays CDK-independent developmental roles in collaboration with tissue-specific transcription factors, including MYOD and neurogenin 2. In mice, p27 interacts functionally with the proneural factor neurogenin 2 in neuronal differentiation (45), and in *Xenopus laevis*, the p27 homolog Xic1 cooperates with the myogenic factor MYOD to mediate myogenesis (46, 47). These effects are cell cycle independent, since a *cdknx* mutant encoding a *xic1* devoid of cyclin-CDK binding restored differentiation defects in *cdknx*-null frogs (46, 47). Tissue differentiation defects in p27-null mice (48–50) are also rescued by p27CK−-knockin (51). These developmental actions may reflect transcriptional roles of p27, whose potential regulation by periodic AKT activation and p27 phosphorylation have yet to be explored. Further evidence for an interaction in transcription came from a ChIP-on-chip survey in NIH 3T3 cells that showed that p27 binds gene promoters in complex with p130, E2F4, HDAC1, and SIN3A (52). This complex appears to mediate *SOX2* repression during ES cell differentiation and in quiescent mouse embryonic fibroblasts (MEFs) (53). A recent genomic survey confirmed broad chromatin association of p27 in quiescent MEFs (54), but biologic targets and function were not characterized.

The present work provides a comprehensive comparison of p27–chromatin binding in human cancer cells with different metastatic potential and reveals the unexpected finding that p27 functionally cooperates with cJun to regulate transcription programs associated with cell adhesion and metastasis. cJun participates in homo- and heterodimeric AP-1 transcription factor complexes to activate drivers of transformation, proliferation, apoptosis, and metastasis in human cancers (30). JNKs phosphorylate and activate cJun (55). cJun regulates EMT during differentiation (55) and drives cancer cell motility and invasion (56), and its levels correlate with poor breast cancer patient outcome (57). Here, we show that cJun interacts with p27 and that its transcriptional activity is importantly regulated by p27. p27 phosphorylation increases its coprecipitation with cJun and cJun activation and increases the magnitude of, and changes the distribution of, cJun/p27 corecruitment to chromatin. A significant proportion of cJun-annotated sites are shared by p27, and cJun recruitment to these sites decreased dramatically with p27 depletion. Thus, p27 phosphorylation may not only promote its interaction with cJun complexes, but also facilitate their stable chromatin association.

Approximately half of p27 binding sites are promoter proximal, and cJun/AP-1 consensus motifs were the most common DNA binding motif. p27 targets in our PI3K-activated lines were nearly twice as abundant as reported in quiescent MEFs (54). The inactivation of PI3K/AKT and the loss of p27pT157pT198 in quiescence (21) may account for these differences. AKT activation is required for G1 to S phase progression, and, in normal mammary epithelial cells, AKT activation and p27 phosphorylation at T157 and T198 peak in mid-G1 (21). Cyclic changes in p27pT157pT198 abundance may modulate p27-regulated transcription across the cell cycle. In cancers with oncogenic PI3K activation, the increased C-terminal p27 phosphorylation may abrogate the corepressive functions of p27 observed in quiescent cells and alter both coregulator and transcriptional target gene selection, directing constitutive p27/cJun association to drive prooncogenic changes in gene expression.

p27 is a central node, integrating PI3K and TGF-β signaling pathways to maintain expression of a profile of EMT genes. Both TGF-β2 and TGF-β2-induced gene profiles are up-regulated in p27-activated models. TGF-β2 is a known EMT driver (58) that promotes metastasis in a variety of malignancies, including gliomas (59) and pancreatic (60, 61) and breast cancers (62). cJun/p27 complexes are corecruited to *TGFB2* to drive its expression as well as associate with chromatin more broadly to modulate transcription of genes critical for cell adhesion, cytoskeletal regulation, and signaling. Metastasis from primary orthotopic tumors was reduced by p27 depletion in 1833 and by *JUN* or *TGFB2* depletion in 231p27CK−DD, supporting the functional importance of these pathways in metastasis.

A large number of cJun/p27 target genes were differentially expressed in p27-activated lines compared with control 231. These cJun/p27 target genes associate with prooncogenic signaling, including p53, cancer-related miRNAs, HIF-1, focal adhesion, and ECM pathways. In addition, in the highly metastatic lines, a new set of target genes were acquired that govern metabolic and HIF-1/hypoxia-regulated pathways. cJun/p27 target genes identified in 231p27CK−DD and 1833, but not activated in 231, may require a threshold of p27 phosphorylation for binding and gene induction. The binding and expression of the validated cJun/p27 targets—*PAI1*/*SERPINE1*, *MYO10*, and *KLF8*—were p27 dependent and increased in metastatic lines. All play roles in EMT or in cancer cell motility and metastasis and are associated with early breast cancer metastasis (31–33).

While cyclin-CDKs have long been known to govern transcription via pRb-family phosphorylation and activation of E2Fs, the present work identifies a novel prooncogenic function for p27 as a transcriptional coregulator of cJun. In over 60% of human cancers, PI3K/AKT constitutively activates effectors AKT, SGK1, and $p90^{RSK1}$, all of which phosphorylate p27 (4, 42). AKT activation is associated with both cytoplasmic p27 (9, 15, 16) and detection of C-terminally phosphorylated p27 in primary human breast cancers (12, 14). That genes differentially regulated by p27 in our cell line models were also differentially expressed in primary breast cancers with high p27pT157 supports the biologic relevance of this mechanism of p27 action in vivo. Moreover, this p27-regulated gene profile is associated with poor cancer survival, indicating its relevance to disease progression. Together, our findings support a model in which C-terminal phosphorylation promotes p27 interaction with cJun, leading to p27/cJun corecruitment to, and activation of, oncogenic genes that drive programs of EMT and cancer metastasis.

Materials and Methods

All materials and methods, including the source of p27 phosphomimetic mutant-expressing cells, lentivirus production and infection, siRNA-mediated knockdown of p27, real-time qPCR, Western blotting, immunoprecipitation, nuclear and cytoplasmic fractionation, transwell invasion assay, ChIP assay, orthotopic xenograft assay, immunohistochemistry, PLA, EMSA, RNA-seq, RNA-seq bioinformatic analysis, ChIP-seq and bioinformatic analysis thereof, analysis of p27-regulated gene expression in primary human breast cancers from TCGA/TCPA, and statistical analysis and references pertaining to these methods are detailed in *SI Appendix, Supplemental Materials and Methods*. Reagents and resources are listed in *SI Appendix*, Table S6. Animal work was compliant with University of Miami Institutional Animal Care and Use Committee.

Data Availability

Data have been deposited in the National Center for Biotechnology Information Gene Expression Omnibus repository under accession no. GSE112446.

ACKNOWLEDGMENTS. This work was supported by the NIH Grant 2R01CA105118-05A1 (to J.M.S.) and by the Department of Defense Breast Cancer Research Program Grant W81XWH-17-1-0456 (to J.M.S. and K.B.). J.M.S., S.A.W., and A.B. were supported by the Doris Duke Charitable Foundation, and K.B. was supported by NIH Grant R01GM113256A1.

1. Koff A, Ohtsuki M, Polyak K, Roberts JM, Massagué J (1993) Negative regulation of G1 in mammalian cells: Inhibition of cyclin E-dependent kinase by TGF-beta. *Science* 260:536–539.
2. Slingerland JM, et al. (1994) A novel inhibitor of cyclin-Cdk activity detected in transforming growth factor beta-arrested epithelial cells. *Mol Cell Biol* 14:3683–3694.
3. Polyak K, et al. (1994) p27Kip1, a cyclin-Cdk inhibitor, links transforming growth factor-beta and contact inhibition to cell cycle arrest. *Genes Dev* 8:9–22.
4. Chu IM, Hengst L, Slingerland JM (2008) The Cdk inhibitor p27 in human cancer: Prognostic potential and relevance to anticancer therapy. *Nat Rev Cancer* 8:253–267.
5. Larrea MD, Wander SA, Slingerland JM (2009) p27 as Jekyll and Hyde: Regulation of cell cycle and cell motility. *Cell Cycle* 8:3455–3461.
6. Mayer IA, Arteaga CL (2016) The PI3K/AKT pathway as a target for cancer treatment. *Annu Rev Med* 67:11–28.
7. Engelman JA (2009) Targeting PI3K signalling in cancer: Opportunities, challenges and limitations. *Nat Rev Cancer* 9:550–562.
8. Chiang GG, Abraham RT (2007) Targeting the mTOR signaling network in cancer. *Trends Mol Med* 13:433–442.
9. Liang J, et al. (2002) PKB/Akt phosphorylates p27, impairs nuclear import of p27 and opposes p27-mediated G1 arrest. *Nat Med* 8:1153–1160.
10. Liang J, et al. (2007) The energy sensing LKB1-AMPK pathway regulates p27(kip1) phosphorylation mediating the decision to enter autophagy or apoptosis. *Nat Cell Biol* 9:218–224.
11. Kossatz U, et al. (2006) C-terminal phosphorylation controls the stability and function of p27kip1. *EMBO J* 25:5159–5170.
12. Motti ML, De Marco C, Califano D, Fusco A, Viglietto G (2004) Akt-dependent T198 phosphorylation of cyclin-dependent kinase inhibitor p27kip1 in breast cancer. *Cell Cycle* 3:1074–1080.
13. Wander SA, et al. (2013) PI3K/mTOR inhibition can impair tumor invasion and metastasis in vivo despite a lack of antiproliferative action in vitro: Implications for targeted therapy. *Breast Cancer Res Treat* 138:369–381.
14. Zhao D, et al. (2015) Cytoplasmic p27 promotes epithelial-mesenchymal transition and tumor metastasis via STAT3-mediated Twist1 upregulation. *Oncogene* 34: 5447–5459.
15. Viglietto G, et al. (2002) Cytoplasmic relocalization and inhibition of the cyclin-dependent kinase inhibitor p27(Kip1) by PKB/Akt-mediated phosphorylation in breast cancer. *Nat Med* 8:1136–1144.
16. Shin I, et al. (2002) PKB/Akt mediates cell-cycle progression by phosphorylation of p27 (Kip1) at threonine 157 and modulation of its cellular localization. *Nat Med* 8: 1145–1152.
17. Hong F, et al. (2008) mTOR-raptor binds and activates SGK1 to regulate p27 phosphorylation. *Mol Cell* 30:701–711.
18. Larrea MD, et al. (2009) RSK1 drives p27Kip1 phosphorylation at T198 to promote RhoA inhibition and increase cell motility. *Proc Natl Acad Sci USA* 106:9268–9273.
19. Fujita N, Sato S, Tsuruo T (2003) Phosphorylation of p27Kip1 at threonine 198 by p90 ribosomal protein S6 kinases promotes its binding to 14-3-3 and cytoplasmic localization. *J Biol Chem* 278:49254–49260.
20. Ciarallo S, et al. (2002) Altered p27(Kip1) phosphorylation, localization, and function in human epithelial cells resistant to transforming growth factor beta-mediated G(1) arrest. *Mol Cell Biol* 22:2993–3002.
21. Larrea MD, et al. (2008) Phosphorylation of p27Kip1 regulates assembly and activation of cyclin D1-Cdk4. *Mol Cell Biol* 28:6462–6472.
22. Besson A, Gurian-West M, Schmidt A, Hall A, Roberts JM (2004) p27Kip1 modulates cell migration through the regulation of RhoA activation. *Genes Dev* 18:862–876.
23. Massagué J (2008) TGFbeta in cancer. *Cell* 134:215–230.
24. Massagué J (2012) TGFβ signalling in context. *Nat Rev Mol Cell Biol* 13:616–630.
25. Kang Y, et al. (2003) A multigenic program mediating breast cancer metastasis to bone. *Cancer Cell* 3:537–549.
26. Vlach J, Hennecke S, Amati B (1997) Phosphorylation-dependent degradation of the cyclin-dependent kinase inhibitor p27. *EMBO J* 16:5334–5344.
27. Taube JH, et al. (2010) Core epithelial-to-mesenchymal transition interactome gene-expression signature is associated with claudin-low and metaplastic breast cancer subtypes. *Proc Natl Acad Sci USA* 107:15449–15454.
28. Minn AJ, et al. (2005) Genes that mediate breast cancer metastasis to lung. *Nature* 436:518–524.
29. Overdevest JB, et al. (2011) CD24 offers a therapeutic target for control of bladder cancer metastasis based on a requirement for lung colonization. *Cancer Res* 71: 3802–3811.
30. Hess J, Angel P, Schorpp-Kistner M (2004) AP-1 subunits: Quarrel and harmony among siblings. *J Cell Sci* 117:5965–5973.
31. Cao R, et al. (2014) Elevated expression of myosin X in tumours contributes to breast cancer aggressiveness and metastasis. *Br J Cancer* 111:539–550.
32. Sternlicht MD, et al. (2006) Prognostic value of PAI1 in invasive breast cancer: Evidence that tumor-specific factors are more important than genetic variation in regulating PAI1 expression. *Cancer Epidemiol Biomarkers Prev* 15:2107–2114.
33. Wang X, et al. (2007) Krüppel-like factor 8 induces epithelial to mesenchymal transition and epithelial cell invasion. *Cancer Res* 67:7184–7193.
34. Connor MK, et al. (2003) CRM1/Ran-mediated nuclear export of p27(Kip1) involves a nuclear export signal and links p27 export and proteolysis. *Mol Biol Cell* 14:201–213.
35. James MK, Ray A, Leznova D, Blain SW (2008) Differential modification of p27Kip1 controls its cyclin D-cdk4 inhibitory activity. *Mol Cell Biol* 28:498–510.
36. LaBaer J, et al. (1997) New functional activities for the p21 family of CDK inhibitors. *Genes Dev* 11:847–862.
37. Grimmler M, et al. (2007) Cdk-inhibitory activity and stability of p27Kip1 are directly regulated by oncogenic tyrosine kinases. *Cell* 128:269–280.
38. Chu I, et al. (2007) p27 phosphorylation by Src regulates inhibition of cyclin E-Cdk2. *Cell* 128:281–294.
39. Besson A, Assoian RK, Roberts JM (2004) Regulation of the cytoskeleton: An oncogenic function for CDK inhibitors? *Nat Rev Cancer* 4:948–955.
40. Besson A, Dowdy SF, Roberts JM (2008) CDK inhibitors: Cell cycle regulators and beyond. *Dev Cell* 14:159–169.
41. Sicinski P, Zacharek S, Kim C (2007) Duality of p27Kip1 function in tumorigenesis. *Genes Dev* 21:1703–1706.
42. Wander SA, Zhao D, Slingerland JM (2011) p27: A barometer of signaling deregulation and potential predictor of response to targeted therapies. *Clin Cancer Res* 17:12–18.
43. Denicourt C, Saenz CC, Datnow B, Cui XS, Dowdy SF (2007) Relocalized p27Kip1 tumor suppressor functions as a cytoplasmic metastatic oncogene in melanoma. *Cancer Res* 67:9238–9243.
44. Wu FY, et al. (2006) Reduction of cytosolic p27(Kip1) inhibits cancer cell motility, survival, and tumorigenicity. *Cancer Res* 66:2162–2172.
45. Nguyen L, et al. (2006) p27kip1 independently promotes neuronal differentiation and migration in the cerebral cortex. *Genes Dev* 20:1511–1524.
46. Vernon AE, Philpott A (2003) A single cdk inhibitor, p27Xic1, functions beyond cell cycle regulation to promote muscle differentiation in Xenopus. *Development* 130: 71–83.
47. Messina G, et al. (2005) p27Kip1 acts downstream of N-cadherin-mediated cell adhesion to promote myogenesis beyond cell cycle regulation. *Mol Biol Cell* 16: 1469–1480.
48. Kiyokawa H, et al. (1996) Enhanced growth of mice lacking the cyclin-dependent kinase inhibitor function of p27(Kip1). *Cell* 85:721–732.
49. Nakayama K, et al. (1996) Mice lacking p27(Kip1) display increased body size, multiple organ hyperplasia, retinal dysplasia, and pituitary tumors. *Cell* 85:707–720.
50. Fero ML, et al. (1996) A syndrome of multiorgan hyperplasia with features of gigantism, tumorigenesis, and female sterility in p27(Kip1)-deficient mice. *Cell* 85: 733–744.
51. Besson A, et al. (2007) Discovery of an oncogenic activity in p27Kip1 that causes stem cell expansion and a multiple tumor phenotype. *Genes Dev* 21:1731–1746.
52. Pippa R, et al. (2012) p27Kip1 represses transcription by direct interaction with p130/E2F4 at the promoters of target genes. *Oncogene* 31:4207–4220.
53. Li H, et al. (2012) p27(Kip1) directly represses Sox2 during embryonic stem cell differentiation. *Cell Stem Cell* 11:845–852.
54. Biçer A, et al. (2017) ChIP-Seq analysis identifies p27(Kip1)-target genes involved in cell adhesion and cell signalling in mouse embryonic fibroblasts. *PLoS One* 12: e0187891.
55. Jochum W, Passegué E, Wagner EF (2001) AP-1 in mouse development and tumorigenesis. *Oncogene* 20:2401–2412.
56. Smith LM, et al. (1999) cJun overexpression in MCF-7 breast cancer cells produces a tumorigenic, invasive and hormone resistant phenotype. *Oncogene* 18:6063–6070.
57. Gee JM, Barroso AF, Ellis IO, Robertson JF, Nicholson RI (2000) Biological and clinical associations of c-jun activation in human breast cancer. *Int J Cancer* 89:177–186.
58. Heldin CH, Vanlandewijck M, Moustakas A (2012) Regulation of EMT by TGFβ in cancer. *FEBS Lett* 586:1959–1970.
59. Kingsley-Kallesen M, Luster TA, Rizzino A (2001) Transcriptional regulation of the transforming growth factor-beta2 gene in glioblastoma cells. *In Vitro Cell Dev Biol Anim* 37:684–690.
60. Schlingensiepen KH, et al. (2011) Transforming growth factor-beta 2 gene silencing with trabedersen (AP 12009) in pancreatic cancer. *Cancer Sci* 102:1193–1200.
61. Cui XP, et al. (2014) HOXA10 promotes cell invasion and MMP-3 expression via TGFβ2-mediated activation of the p38 MAPK pathway in pancreatic cancer cells. *Dig Dis Sci* 59:1442–1451.
62. Beisner J, et al. (2006) A novel functional polymorphism in the transforming growth factor-beta2 gene promoter and tumor progression in breast cancer. *Cancer Res* 66: 7554–7561.